Abundant expression of the membrane-anchored protease-regulator RECK in the anterior pituitary gland and its implication in the growth hormone/insulin-like growth factor 1 axis in mice

AUTHOR(S):

Ogawa, Shuichiro; Matsuzaki, Tomoko; Noda, Makoto

CITATION:

Ogawa, Shuichiro ...[et al]. Abundant expression of the membrane-anchored protease-regulator RECK in the anterior pituitary gland and its implication in the growth hormone/insulin-like growth factor 1 axis in mice. Molecular and Cellular Endocrinology 2020, 508: 110790.

ISSUE DATE:

2020-05-15

URL:

http://hdl.handle.net/2433/254484

Molecular and Cellular Endocrinology 508 (2020) 110790

Contents lists available at ScienceDirect

Molecular and Cellular Endocrinology

journal homepage: www.elsevier.com/locate/mce

Abundant expression of the membrane-anchored protease-regulator RECK in the anterior pituitary gland and its implication in the growth hormone/insulin-like growth factor 1 axis in mice

Shuichiro Ogawa, Tomoko Matsuzaki, Makoto Noda*

Department of Molecular Oncology, Kyoto University Graduate School of Medicine, Yoshida-Konoe-cho, Sakyo-ku, Kyoto, 606-8501, Japan

ARTICLE INFO

Keywords:
RECK
Somatotroph
Growth hormone
Insulin-like growth factor 1
Growth hormone releasing hormone receptor
Growth hormone secretagogue receptor
Growth hormone receptor

ABSTRACT

The tumor suppressor gene *Re*version-inducing *c*ysteine-rich protein with *K*azal motifs (*Reck*) encodes a membrane-anchored protease regulator expressed in multiple tissues in mouse embryos and is essential for embryonic development. In postnatal mice, however, physiological roles for the RECK protein remain unclear. We found in this study that *Reck* is abundantly expressed in growth hormone (GH)-producing cells (somatotrophs) in the anterior pituitary gland (AP). We also found that two types of viable *Reck* mutant mice, one with reduced RECK expression (Hypo mice) and the other with induced *Reck* deficiency from 10 days after birth (iKO mice treated with tamoxifen), exhibit common phenotypes including decreases in body size and plasma levels of insulin-like growth factor-1 (IGF1). To gain insights into the function of RECK in the AP, we characterized several somatotroph-associated molecules in the AP of these mice. Immunoreactivity of GH was greatly reduced in tamoxifen-treated iKO mice; in these mice, two membrane receptors involved in the stimulation of GH secretion [growth hormone secretagogue receptor (GHSR) and growth hormone releasing hormone receptor (GHRHR)] were decreased, however, their mRNAs were increased. Decrease in GHSR immunoreactivity and concomitant increase in its mRNA were also found in the other mutant line, Hypo. Furthermore, reduced immunoreactivity of growth hormone receptor (GHR) and concomitant increase in its mRNA was also found in the liver of Hypo mice. These results raise the possibility that RECK supports proper functioning of the GH/IGF1 axis in mice, thereby affecting their growth and metabolism.

1. Introduction

*Re*version-inducing *C*ysteine-rich protein with *K*azal motifs (*RECK*) was initially isolated as a transformation suppressor gene encoding a glycosylphosphatidylinositol (GPI)-anchored glycoprotein (Takahashi et al., 1998). Subsequent studies revealed that the RECK protein negatively regulated several matrix metalloproteinases, preventing degradation of cell surface proteins and promoting the accumulation of extracellular matrix (ECM) (Oh et al., 2001; Noda et al., 2003; Omura et al., 2009; Matsuzaki et al., 2018a). *RECK* expression is down-regulated in a wide variety of tumors, leading to increases in their angiogenesis-inducing activity and their potential for invasion, metastasis, and recurrence (Noda and Takahashi, 2007; Hill et al., 2011; Shi et al., 2016).

Reck-deficient mice die around embryonic day 10.5 (E10.5) with increased gelatinase activity in the tissue, decreased tissue integrity, and abnormalities in vascular and neural development (Oh et al., 2001; Chandana et al., 2010; Almeida et al., 2015). Studies on the vascular phenotype of these mice revealed that RECK binds GPR124, an orphan G-protein coupled receptor (GPCR), and WNT7 to promote the ligand-specific canonical WNT signaling required for brain angiogenesis (Ulrich et al., 2016; Vanhollebeke et al., 2015; Noda et al., 2016; Cho et al., 2017; Eubelen et al., 2018; Vallon et al., 2018). A study on the neural phenotype of *Reck*-deficient mice, revealed that RECK also promotes Notch signaling required for proper neurogenesis by inhibiting protease-mediated shedding of Notch-ligands on adjacent cells (Muraguchi et al., 2007). Thus, molecular functions of RECK elucidated by studying mouse phenotypes include protease regulation and enhancement of WNT and Notch signaling. The elucidation of physiological roles for RECK in postnatal life, however, had been hindered by the embryonic lethality of *Reck*-deficient mice.

In the present study, to investigate postnatal activities of RECK, we searched for tissues expressing *Reck* in adult mice and found that a large fraction of pituitary somatotrophs express *Reck*. Notably, growth

* Corresponding author. Kyoto University Graduate School of Medicine, Yoshida-Konoe-cho, Sakyo-ku, Kyoto, 606-8501, Japan
E-mail address: noda.makoto.3x@kyoto-u.ac.jp (M. Noda).

https://doi.org/10.1016/j.mce.2020.110790
Received 16 October 2019; Received in revised form 4 March 2020; Accepted 8 March 2020
Available online 09 March 2020

List of Abbreviations

AP	(anterior pituitary gland)
ARH	(arcuate nucleus of the hypothalamus)
CreERT2	(Tamoxifen-dependent Cre recombinase 2)
ECM	(extracellular matrix)
GH	(growth hormone)
GHR	(growth hormone receptor)
GHRH	(growth hormone releasing hormone)
GHRHR	(growth hormone releasing hormone receptor)
GHRP-2	(growth hormone-releasing peptide-2)
GHSR	(growth hormone secretagogue receptor/ghrelin receptor)
GPCR	(G protein-coupled receptor)
Hypo	(hypomorph)
IGF1	(insulin-like growth factor 1)
IGFBP3	(insulin-like growth factor binding protein 3)
iKO	(inducible knockout)
mT	[membrane-targeted tandem dimer Tomato (a red fluorescent protein)]
mG	(membrane-targeted green fluorescent protein)
PRL	(prolactin)
RECK	(reversion-inducing cysteine rich protein with Kazal motifs)
SMA	(smooth muscle actin)
SST	(somatostatin)
SSTR	(somatostatin receptor)
TAX	(tamoxifen)
TSH	(thyroid-stimulating hormone)

hormone (GH) is produced mainly by somatotrophs in the anterior pituitary gland (AP). GH not only increases bone length, bone density, and muscle mass in young animals, but also regulates lipid and carbohydrate metabolism and water retention (Ranke and Wit, 2018). GH-production in the AP is regulated positively by growth hormone releasing hormone (GHRH) and negatively by somatostatins (SSTs); these regulatory peptides are produced by hypothalamic neurons and reach the AP through local blood vessels. GHRH and SSTs bind cognate GPCRs (GHRHR and SSTRs, respectively) present on the surface of somatotrophs (Ben-Shlomo and Melmed, 2010; Eigler and Ben-Shlomo, 2014; Fridlyand et al., 2016). Another stimulatory GPCR, growth hormone secretagogue receptor (GHSR), is also expressed in somatotrophs, but its ligand, ghrelin, is mainly produced by the gastrointestinal tract, increasing after fasting and serving as an orexigenic hormone (Kojima et al., 1999; Kojima and Kangawa, 2005). Gastrointestinal ghrelin is known to transmit its signal via vagal afferent nerves (Date et al., 2002, 2006). Ghrelin is also produced by the AP, and such local ghrelin may act as a paracrine factor enhancing GHRH signaling in somatotrophs (Howard et al., 1996; Denef, 2008).

The growth-promoting activity of GH is primarily mediated by insulin-like growth factor-1 (IGF1; also known as somatomedin-1 or –C) secreted from the liver in response to GH (Laron, 1999). Growth hormone receptor (GHR), a cytokine-receptor-type single-pass transmembrane receptor, is expressed in the liver and transduces multiple downstream signals and evokes IGF1 secretion (Melmed, 2016; Dehkhoda et al., 2018). IGF1 stimulates cell proliferation and survival in various tissues, including those rich in ECM such as skeletal muscle, cartilage, bone, and skin. IGF1 also acts as a feedback regulator suppressing GH production (Berelowitz et al., 1981; Yamashita and Melmed, 1987; Wallenius et al., 2001; Sjogren et al., 2002).

Various components of this endocrine cascade, termed the GH/IGF1 axis (see Fig. 6b), are major targets of mutations causing growth retardation (Pilecka et al., 2007; Dauber et al., 2014; Gahete et al., 2016; Ranke and Wit, 2018). In contrast, overproduction of GH due, for example, to benign pituitary tumors may cause gigantism in children and acromegaly in adults (Melmed, 2011, 2016). Specific agonists or antagonists of receptors involved in the GH/IGF1 axis are of potential therapeutic and/or diagnostic value. Successful examples include GHRP-2, a synthetic GHSR agonist (i.e, a ghrelin analogue) that stimulates GH production (Peroni et al., 2012), and Octreotide, a potent SSTR2 agonist (i.e, a somatostatin analogue) that suppresses GH production (Gadelha et al., 2012) (see Fig. 6b).

In this study, we characterized the phenotypes of three lines of viable *Reck* mutant mice, two with reduced RECK expression ($Reck^{+/-}$ and Hypo mice expressing RECK at 50% and 20% of the normal level, respectively) and a third line (termed iKO) in which the majority of *Reck* can be deleted after birth by treatment with tamoxifen (TAX). Although $Reck^{+/-}$ mice are normal in body size, the other two lines, Hypo and TAX-treated iKO mice, were found to exhibit reduced body weight and body length. These findings prompted us to compare [1] the level of circulating IGF1, [2] the level of GH and its changes in response to fasting, GHRP-2, and Octreotide, and [3] the level of several membrane receptors involved in the GH/IGF1 axis in the AP and the liver of these mice. Our data support the idea that RECK helps sustain the expression of membrane receptors involved in the GH/IGF1 axis in mice, thereby promoting their body growth.

2. Materials and methods

2.1. Mice

Animal experiments were approved by the Animal Experimentation Committee, Kyoto University and conducted in accordance with its regulations. To visualize *Reck*-expressing cells, we used two lines of *Reck*-reporter mice (Fig. S1): (1) $Reck^{CreERT2/+}$;R26R mice obtained by crossing $Reck^{CreERT2}$ [tm3.1(CreERT2)Noda] mice (Matsuzaki et al., 2018b) with R26R mice (Soriano, 1999) and (2) $Reck^{CreERT2/+}$;mTmG mice obtained by crossing $Reck^{CreERT2}$ mice with *mTmG* mice (Muzumdar et al., 2007). In both lines, RECK expression can be visualized after treatment with tamoxifen (TAX; Sigma, T5648). Injection of TAX (0.05 mg/g-body weight; once a day for 5 days) was started from 9 weeks after birth. The animals were euthanized at 10 weeks after birth, and marker (LacZ or mG) expression was examined. The *Reck* mutant alleles $Reck^{flex1}$ (tm2.1Noda, RRID:IMSR_RBRC10232), $Reck^{-}$ (tm2.2Noda, RRID:IMSR_RBRC10233; previously termed $Reck^{\Delta}$), and $Reck^{Low}$ (tm1Noda, RRID:IMSR_RBRC10232; referred to as $Reck^{L}$ in this paper) have been described elsewhere (Yamamoto et al., 2012). The $Reck^{L/-}$ mice [termed Hypo in this manuscript; Fig. S2b(4)] were generated by crossing $Reck^{Low/Low}$ and $Reck^{+/-}$ mice. The $Reck^{L/+}$ mice (RECK level: ~70% of normal) obtained from this cross were normal in body weight (Fig. S6a, bar 2) and hence used as the littermate controls for the Hypo mice in relevant experiments. Postnatal inactivation of the *Reck* gene was induced in iKO ($Reck^{flex1/CreERT2}$ obtained by crossing $Reck^{flex1}$ with $Reck^{CreERT2}$) mice [Fig. S2b(5)] by intra-peritoneal injection of TAX (0.05 mg/g-body weight) dissolved in corn oil (Nacalai, 25,606–65) on four consecutive days from P10 to P13. Body length was determined as the distance between the nose and anus.

2.2. Histology

For whole-mount X-gal staining, resected organs were fixed in rinse solution [phosphate buffered saline (PBS) supplemented with 0.02% NP40 and 0.01% deoxycholate] containing 2% paraformaldehyde (PFA) and 0.2% glutaraldehyde at 4 °C overnight, washed with the rinse solution (15 min, 3 times), then incubated in PBS containing 5 mM $K_3Fe(CN)_6$, 5 mM $K_4Fe(CN)_6$, 0.02% NP40, 0.01% deoxycholate, 2 mM $MgCl_2$, 5 mM EGTA, and 1 mg/L X-gal at 37 °C for 16 h. For X-gal staining of tissue slices, the fixed organs were transferred into 30%

sucrose for cryoprotection, embedded in OCT compound (Sakura Finetek, Japan), frozen at −80 °C, and sectioned (5 μm-thick) with a Cryostat (CM1850, Leica, Japan), and stained with X-gal as described above, followed by nuclear counterstaining with 0.1% Nuclear fast red. For Hematoxylin-Eosin (HE) staining, resected organs were fixed in 4% PFA at 4 °C overnight, cryosectioned as outlined above, and stained with hematoxylin and eosin.

2.3. Immunofluorescence staining

Tissue sections (5 μm) were incubated in PBS containing 10% goat serum at room temperature (RT) for 1 h to block non-specific antibody binding, incubated with primary antibodies at 4 °C for 16 h, washed with PBS, and then incubated with secondary antibodies at RT for 1h. After washing and nuclear counter-staining with Hoechst 33,342 (DOJINDO, Japan), sections were mounted with Fluoromount (K024, Diagnostic Biosystems) and observed with a fluorescence microscope (BZ-9000, Keyence, Japan). Primary antibodies (Table S1): GH (AbD, 4750–5059), PRL (AbD, 7770–2949), TSH (AbD, 8922–6009), ACTH (Abcam, ab74976), SMA (DAKO, MO85), CD31 (BD Pharmingen, 550,274), Nestin (SANTA CRUZ, C2007), SSTR2A (Gramsch Laboratories, SS-800), SSTR5 (Abcam, ab156864), GHRHR (Abcam, ab76263), GHSR (Abcam, ab95250), GHR (Abcam, ab134078), and RECK (see legend to Fig. S3). Secondary antibodies: Cy5-conjugated AffiniPure Goat Anti-Rat IgG(H + L) (Jackson IR #112-175-062) for anti-CD31 and goat anti-rabbit IgG CF647 (Biotium, 20043) for the other antibodies.

2.4. Image analysis

To identify *Reck*-expressing cells in the AP, pituitary slices from TAX-treated $Reck^{CreERT2/+}$;*mTmG* mice were immunostained for a cell type marker and recorded on 3 channels: far red (antigen), green (RECK), and blue (nuclei). The cells positive for each color and the cells doubly positive for far-red and green were counted using Fiji software. For semi-quantification of receptor proteins, immunofluorescence images (×400 magnification) acquired under equivalent conditions from either the ventral side of the AP (6 images per slice) or from the liver, using the same area in the same lobe of the livers of the mice (12 images per slice) were stored in TIFF format and subjected to image analysis using Fiji software to quantify the number of nuclei and the intensity of far red fluorescence (i.e., immunoreactivity). In every experiment, two control slices (AP from wild type mice) stained with secondary antibodies alone were included and subjected to image analysis in parallel with the test animals. The intensity of far-red fluorescence was divided by the number of nuclei to obtain the raw value of immunoreactivity per cell (IR/C). The average raw IR/C of the control slices (i.e., background fluorescence) was subtracted from that of each group of experimental slices to obtain the calibrated IR/C (termed “IHC signal” in the Figures).

2.5. Plasma preparation and ELISA

Wild type and *Reck* mutant mice (all in a C57BL/6J background, 2–5 months old) were anesthetized with isoflurane (inhalation) just before injection of GHRP-2 (Kaken; 20 mg/kg-body weight, i.v.) or Octreotide (Novartis; 1 mg/kg-body weight, s. c.). Animals were fasted for 16 h before injection of GHRP-2. Whole blood was collected from the tail tip before and 30-min after peptide injection and centrifuged in EDTA-coated tubes to separate the cells. The supernatant (plasma) was stored at −80 °C until use. The levels of GH, IGF1, and IGFBP3 in the plasma were determined using ELISA kits (GH: EZRMGH-45K, Merck Millipore; IGF1: MG100, R&D; IGFBP-3: MGB300, R&D) following the manufacture's protocols. The sensitivity (the lowest detectable level), intra-assay CV%, and inter-assay CV% of the kits are as follows: GH (0.07 ng/ml, 2.6%, 4.2%), IGF1 (1.6 pg/ml, 4.3%, 6.0%), IGFBP-3 (2.74 pg/ml, 4.8%, 7.2%).

2.6. Immunoblot assay

In the experiments shown in Figs. 4m and 4o, one pituitary gland was suspended in 30 μl lysis buffer containing 50 mM Tris pH 7.5, 0.5 M NaCl, 1% NP40, 0.1% SDS, 0.5% deoxycholate, 5 mM N-ethylmaleimide, and 20x Protease inhibitor cocktail (03969, Nakarai, Japan), homogenized by vigorous shaking with silicon beads (2 mm Φ) using ShakeMan (BMS, Japan) for 15 s, followed by sonication (UR-20P, TOMY, Japan) for a total of 10 s on ice. After 10 min centrifugation (16,500 × *g*) at 4 °C, the supernatant was separated, mixed with 10 μl 4x Laemmli sample buffer (without reducing agent), and incubated at room temperature for 5 min before SDS-PAGE (one pituitary per lane). Immunoblot assays were performed using anti-GHRHR or anti-GHSR antibodies (Table S1) as primary antibodies, HRP-conjugated goat anti-Rabbit IgG (Santa Cruz) as secondary antibodies, and GAPDH (V-18) HRP (sc-20357, SantaCruz) as the internal control.

2.7. qRT-PCR

Total RNA was extracted from tissues using NucleoSpin RNA (MACHEREY-NAGEL) for liver RNA and ReliaPrep RNA Cell Miniprep System (Promega, Z6011) for pituitary RNA. qRT-PCR was performed with the Mx3005P QPCR System (Stratagene) using GoTaq Probe 1-Step RT-qPCR System (Promega, A6120) for mouse *Reck* and GoTaq 1-Step RT-qPCR System (Promega, A6020) for mouse *Ghrhr*, *Ghsr*, *Sstr2*, *Sstr5*, *Ghr*, *Mars*, and *Gapdh*. Primers for qRT-PCR are listed in Table S2.

2.8. Statistics

Quantitative data are presented as mean ± s.e.m. Comparison between two groups was performed using the F-test and Student's T-test in Excel. Comparison among more than two groups was performed using the Bartlett's test to assess homogeneity of variance and the Welch's *t*-test and One-way ANOVA to assess differences in the mean values when the variance was homogeneous; when the variance was heterogeneous, Welch's *t*-test and the Kruskal-Wallis test followed by the Mann-Whitney *U* test with Bonferroni correction was used to assess the significance of differences. P values < 0.05 were considered significant.

3. Results

3.1. Reck-expressing cells are found in the ARH and AP in adult mice

To investigate the functions of RECK in adult mice, we visualized *Reck*-expressing cells *in vivo* using two lines of *Reck*-reporter mice: β-gal-reporter (Fig. S1a) and FL-reporter mice (Fig. S1b). In both lines, *Reck*-expressing cells can be visualized after tamoxifen (TAX)-treatment which triggers the nuclear translocation of CreERT2 recombinase, consequent excision of the intervening poly-A signal, and expression of the marker gene (Fig. S1). In the β-gal reporter mouse ($Reck^{CreERT2/+}$;*R26R*), TAX-treatment followed by X-gal staining results in blue signals in *Reck*-expressing cells [Fig. S1a; Fig. S2a(1)]. In the FL-reporter mouse ($Reck^{CreERT2/+}$;*mTmG*), *Reck*-expressing cells emit green fluorescence after TAX-treatment on a background of the other cells emitting red fluorescence [Fig. S1b; Fig. S2a(2)].

These reporter systems are not as efficient as immunohistochemical staining and *in situ* hybridization (see below, also see Fig. S1), but they allow gene expression to be directly and clearly visualized, even in whole-mount tissue samples. In a previous study using these reporter mice, we found that *Reck*-expression was generally low in the adult mouse brain but upregulated in the hippocampus after transient cerebral ischemia (Matsuzaki et al., 2018b). In the present study, we found strong signals in two sites in the ventral part of the brain: the arcuate

nucleus of the hypothalamus (ARH; Fig. 1a and b) and the pituitary gland (Fig. 1c). The signals in the pituitary gland were abundant mainly in the AP (Fig. 1d and e) where various hormone-producing cells reside. We therefore set out to determine the identity of these cells.

We first estimated the labeling efficiency of RECK in adult FL-reporter mice. Nine-week old FL-reporter mice were treated with TAX for one week to permit the expression of mG in RECK expressing cells (Fig. S1b; Fig. S3a). Mice were then euthanized and pituitary slices were prepared and subjected to immunofluorescence staining (IF) with rabbit anti-RECK antibodies (Fig. S3a, magenta signals). Morphometric quantification indicated that ~74% of all AP cells were positive for RECK-immunoreactivity (Fig. 2a, bar 1) and ~45% were also positive for green fluorescence (Fig. 2a, bar 2). Of note, green cells are almost always positive for magenta in the merged images (Fig. S3a, panel 6), indicating that ectopic GFP expression is rare in this system, and that RECK-positive cells identified by Cre-mediated recombination are also identified as RECK-positive cells by immunohistochemistry. Thus, a rough estimate of the labeling efficiency of RECK-positive cells in this system is ~61% (i.e., 45/74). Although the efficiency is moderate, this system is the best choice for double labeling, since the antibodies against RECK and most of the AP cell-type markers (see below) are of rabbit origin (Table S1), making it difficult to perform double immunofluorescence staining.

Thus, we performed immunofluorescence staining of pituitary slices prepared from FL-reporter mice. Mice were treated with TAX from week 9 to label *Reck*-expressing cells with mG, and the mice were euthanized and pituitary slices were prepared at week 10. The six major cell types found in the AP were identified using antibodies against growth hormone (GH), prolactin (PRL), thyroid stimulating hormone (TSH), smooth muscle actin (SMA; vascular smooth muscle cells), CD31 (vascular endothelial cells), or Nestin (Fig. 2b; Fig. S3b). Among the hormone-producing cells in the AP, GH-positive cells (somatotrophs) are the most abundant (~50%) and PRL-positive (15–20%) and TSH-positive cells (~5%) are less abundant (Mitrofanova et al., 2017). We counted the nuclei (blue) and immunoreactive cells (magenta) in images such as those shown in Fig. 2b to estimate the proportion of each cell type (Fig. 2c). Our data are largely consistent with those in the literature and indicate that the proportion of GH-positive cells in this region is ~54% (Fig. 2c, bar 2). We also counted green-magenta doubly positive cells to estimate [1] the proportion of each cell type among the *Reck*-expressing cells (Fig. 2d) and [2] the relative abundance of *Reck*-expressing cells in each cell type (Fig. 2e). Our data indicate that a large proportion of *Reck*-expressing cells in the AP are somatotrophs (Fig. 2d) and that the majority of somatotrophs express *Reck* (Fig. 2e, bar 1).

3.2. Phenotypes of Reck mutant mice

Reck is essential for mouse embryogenesis (Oh et al., 2001). To investigate the functions of *Reck* in postnatal mice, we examined the properties of three viable *Reck* mutant lines with different RECK expression levels and/or different timing of *Reck* reduction (Fig. 3a). The first line, *Reck*-null heterozygote ($Reck^{+/-}$), expresses RECK at ~50% of the normal level throughout life [Fig. S2b(3)]. The second line, Hypo ($Reck^{L/-}$), expresses RECK at ~20% of the normal level throughout life [Fig. S2b (4)] (Yamamoto et al., 2012). The third line, iKO ($Reck^{CreERT2/flex1}$), is newly developed in this study: this line originally expresses RECK at ~50% of the normal level, but after TAX-treatment, the *Reck* gene is inactivated in the cells that are competent to express *Reck* [Fig.

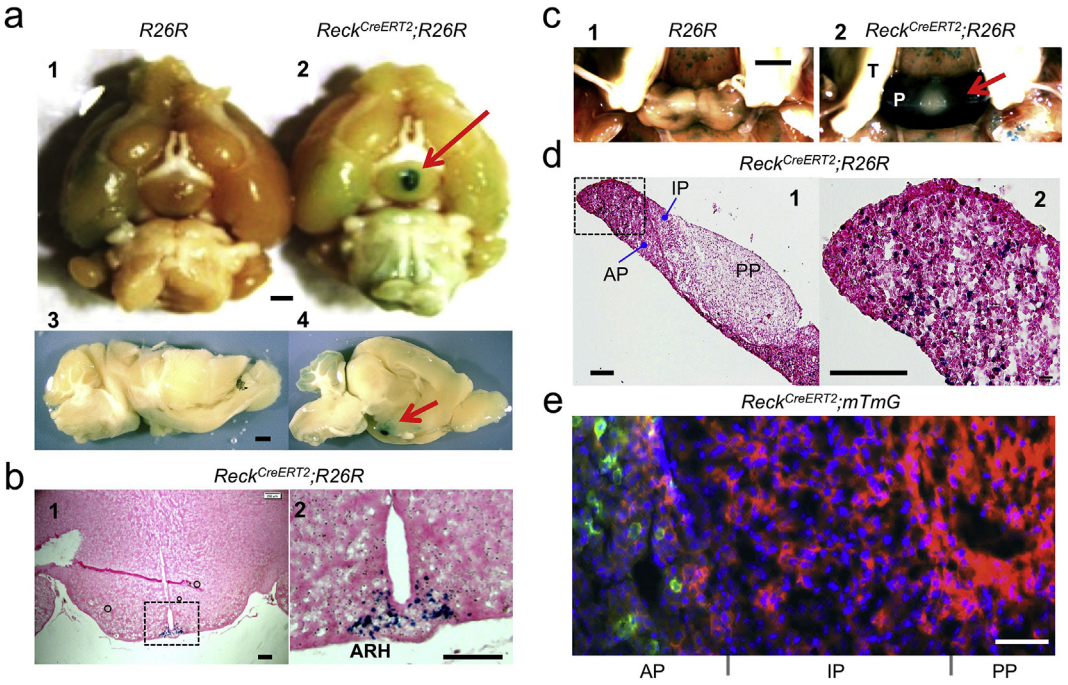

Fig. 1. *Reck*-expressing cells in adult mice. (a) Ventral view of the whole brain (1, 2) and sagittal cross sections of the brain (3, 4) from *R26R* mice (1, 3; background control) and $Reck^{CreERT2/+}$;*R26R* mice (2, 4; β-gal reporter mouse) treated with TAX from 9 weeks (5 times, every 24 h) and euthanized at 10 weeks after birth. Samples were subjected to X-gal staining (blue signals) to detect *Reck*-expressing cells. Red arrow: a prominent cluster of blue signals. **(b)** Coronal section focusing on the hypothalamic region of the brain from a $Reck^{CreERT2/+}$;*R26R* mouse after X-gal staining (blue) and nuclear counter-staining (red). A magnified view of the boxed area in panel 1 is shown in panel 2. Note the prominent cluster of blue signals in the arcuate nucleus of the hypothalamus (ARH). **(c)** Pituitary gland of an *R26R* mouse (1; background control) and a $Reck^{CreERT2/+}$;*R26R* mouse (2; β-gal reporter mouse) after X-gal staining. T: trigeminal nerve. P: pituitary gland. Note the intense blue signals in the pituitary gland of β-gal reporter mouse (red arrow in 2). **(d)** Section of the pituitary gland from a $Reck^{CreERT2/+}$;*R26R* mouse after X-gal staining (dark blue) and nuclear counter-staining (red). AP: the anterior pituitary. IP: the intermediate lobe of the pituitary. PP: the posterior pituitary. Magnified view of the boxed area in panel 1 is shown in panel 2. **(e)** Fluorescent micrograph of a section of the pituitary gland from a $Reck^{CreERT2/+}$;*mTmG* mouse treated with TAX from 9 weeks (5 times, every 24 h) and euthanized at 10 weeks after birth. Green: *Reck*-expressing cells. Red: other cells. Blue: nuclei. Note the green cells abundant in the AP. Scale bar: 1 mm in **a** and **c**, 200 μm in **b** and **d**, 50 μm in **e**.

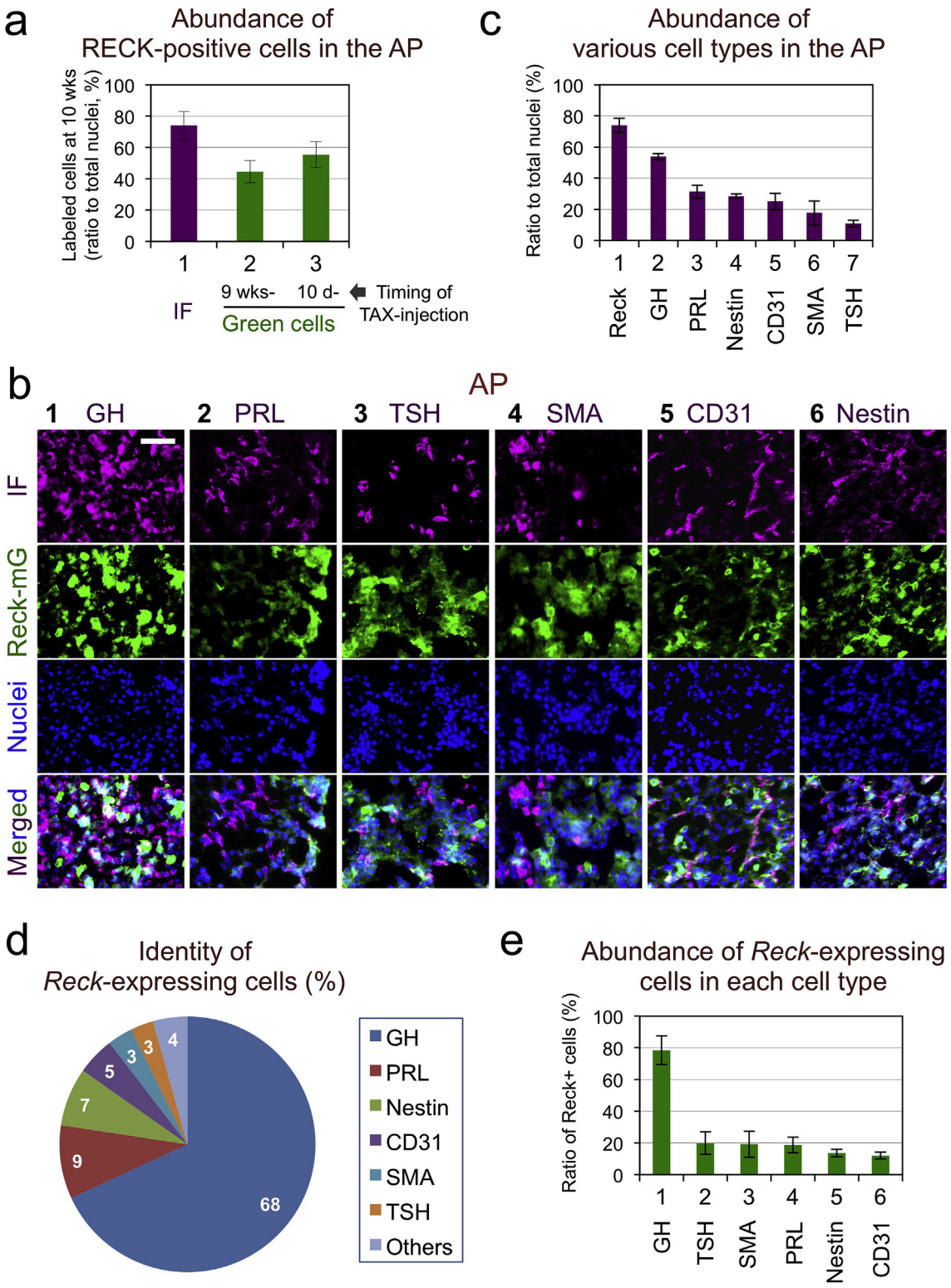

Fig. 2. Abundance and identity of *Reck*-expressing cells in the AP. (a) Abundance of RECK-positive cells. Bar 1: abundance assessed by immunofluorescence staining with anti-RECK antibodies (Fig. S3a, panels 4 and 6). Bar 2: abundance assessed by CreERT2-mediated reporter gene expression in an FL-reporter mouse (female, 10-weeks old) treated with TAX starting from 1 week before dissection (5 times, every 24 h; Fig. S3a, panels 2 and 6). Bar 3: abundance assessed in an FL-reporter mouse (female, 8-weeks old) treated with TAX from day 10–13 after birth (4 times, every 24 h; Fig. S4b, panels 1 and 3). Note that ~74% of all AP cells were RECK-immunoreactive (bar 1), and among them, ~61% (i.e., 45/74) emitted green fluorescence after 1-week pulse labeling (bar 2) and ~74% (i.e., 55/74) emitted green fluorescence after early treatment (bar 3). **(b)** Typical images of pituitary sections of pulse (1-week)-labeled $Reck^{CreERT2/+}$;*mTmG* mice after immunoflorescence (IF) staining with antibodies against various AP cell markers. The top panel in each column (magenta) shows the IF image for the indicated antigen, the second panel shows *Reck*-expressing cells (green), the third panel shows nuclei (blue), and the bottom panel shows the overlay of the above three images in which magenta-green doubly positive cells are white. Scale bar: 50 μm. **(c–e)** Quantitative analyses of images as shown in **b**. The number of nuclei, IF-positive cells, *Reck*-positive cells, and doubly positive cells were counted using Fiji software. The ratios of IF-positive cells to the nuclei **(c)**, the relative frequency of the cells positive for each marker among the *Reck*-positive cells **(d)**, and the frequency of *Reck*-positive cells among each cell type **(e)** are presented as mean ± sem (n = 4). Virtually no overlap was found between the cells positive for S100B (a folliculo-stellate cell marker) and *Reck*-positive cells (data not show).

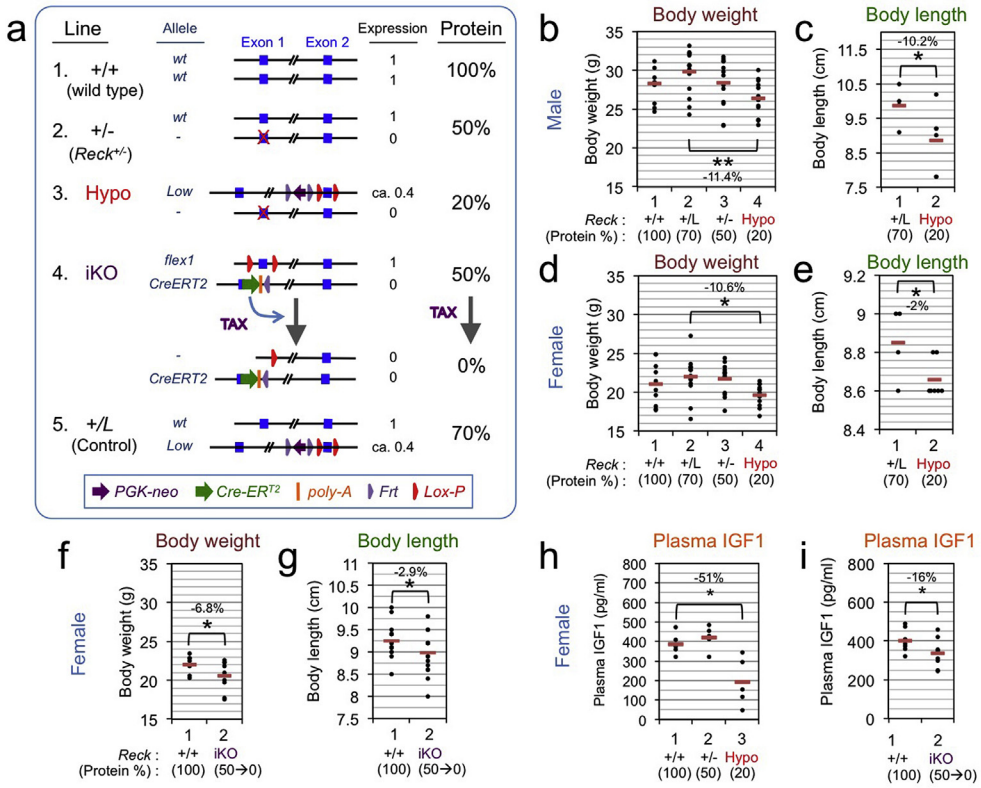

Fig. 3. Phenotypes of viable *Reck* mutant mice. (a) Allele composition of *Reck* mutant mice used in this study. Symbols used in the allele diagrams are explained in the bottom box. The theoretical RECK protein level expressed in each line, relative to the normal level, is given on the right hand side. **(b)** Body weights of four groups of male mice (~10 weeks old) with different RECK expression levels. See panel **a** for allele composition of each group of mice. n = 20 (+/+), 15 (+/L), 15 (+/−), 14 (Hypo). **(c)** Body lengths of two groups of male mice (~10 months old) with different RECK expression levels. n = 4 (+/L), 6 (Hypo). **(d)** Body weights of four groups of female mice (~10 weeks old) with different RECK expression levels. n = 10 (+/+), 14 (+/L), 13 (+/−), 14 (Hypo). **(e)** Body lengths of two groups of male mice (~10 months old) with different RECK expression levels. n = 4 (+/L), 7 (Hypo). **(f)** Body weights of female wild type mice (group 1) and TAX-treated iKO mice (group 2) at ~10 weeks after birth. n = 7 (+/+), 9 (iKO). **(g)** Body lengths of female wild type mice (group 1) and TAX-treated iKO mice (group 2) at ~10 months after birth. n = 15 (+/+), 16 (iKO). **(h, i)** Plasma IGF1 in mice with different RECK expression levels. **(h)** Comparison between +/+, +/−, and Hypo female mice at 18 weeks after birth. n = 5 (+/+), 6 (+/−), 5 (Hypo). **(i)** Comparison between wild type and iKO female mice at 15–18 weeks after birth. n = 7 (+/+), 9 (iKO). In **b-i**, dots represent individual animals and the horizontal bar shows the average of each group. Relative level of RECK protein (in %) is given in the bottom parenthesis. Differences between groups (%) and the significance (*p < 0.05, **p < 0.01) are shown in panels **b-g**.

S2b (5)]. In this mutant, *Reck*-knockout can be induced at any time, and the risk of inducing developmental abnormalities (Forni et al., 2006; Higashi et al., 2009) by systemic overexpression of CreERT2 recombinase is diminished. iKO mice were found to be viable and show no gross phenotype when treated with TAX as early as day 10–13 after birth (P10 – P13). To estimate the efficiency of induced *Reck* gene deletion in this mutant, we treated adult FL-reporter mice (*Reck*$^{CreERT2/+}$;*mTmG*) with TAX from P10 to P13 and euthanized the mice at 10 weeks (Fig. S4). Morphometry indicated that about 55% of all AP cells were positive for green fluorescence (Fig. 2a, bar 3). As mentioned above, ~74% of all AP cells were positive for RECK-immunoreactivity at this age (Fig. 2a, bar 1). Thus, TAX treatment causes recombination in about 74% (=55/74) of RECK:CreERT2 expressing cells. Assuming that the efficiency of TAX-mediated nuclear translocation of CreERT2 and CreERT2-mediated DNA recombination is similar in FL-reporter mice and iKO mice, then the efficiency of *Reck* deletion in iKO mice treated with TAX will also be about 74%, generating mice which express RECK at about 13% of normal: iKO mice are RECK haploids and express RECK at 50% of normal. TAX-treatment deletes the *RECK* gene from approximately 74% of the RECK expressing cells. Therefore, approximately 26% of the original RECK expressing cells continue to be RECK haploids, with each cell expressing RECK at 50% of normal.

As reported previously, Hypo mice show limb abnormalities (Yamamoto et al., 2012). We found in this study that adult Hypo mice (both male and female) have lower body weights (Fig. 3b, d, group 4; Fig. S5a, b, red dots) and body lengths (Fig. 3c, e, group 2) than their littermate controls. In contrast, TAX-treated iKO mice have no obvious developmental abnormalities, but they show a mild but significant reduction in their body weights and body lengths compared to their littermate controls (Fig. 3f and g, group 2; Fig. S5c, d, purple dots). There were no significant differences in body weight between +/+, *L*/+ (expected RECK level: ~70% of normal), and +/- mice (RECK level: 50% of normal) (Fig. S6a). Taken together, these findings suggest that *Reck* might affect the body size of mice.

Somatotrophs produce GH, and GH induces IGF1 secretion from the liver to promote somatic growth. IGF1 is used to screen for GH abnormality in the clinic: GH secretion is pulsatile in nature and is affected by many factors such as sleep, feeding, and exercise, whereas IGF1 levels do not undergo such short-term fluctuations (Ketha and Singh, 2015). We therefore determined the concentration of circulating IGF1 in these mice (Fig. 3h and i). The level of plasma IGF1 was clearly lower in Hypo mice and mildly lower in TAX-treated iKO mice compared to normal mice. These results suggest that GH secretion is abnormal in Hypo and TAX-treated iKO mice, raise the possibility that RECK has a positive effect on GH secretion.

The secretory pattern of GH differs between the sexes; in males it is more pulsatile than in females (Jansson et al., 1985). Therefore, since we found that *Reck* mutations affect body size in both males and females (Fig. 3b–e; Fig. S5), we chose to focus on female animals in the rest of this study.

3.3. Somatotrophs and GH in mice with reduced RECK expression

To test the possibility that RECK directly affects somatotrophs, we stained pituitary slices prepared from normal mice and the three *Reck* mutant lines (see Fig. 3a and Fig. S2b) with anti-GH antibodies (representative images are shown in Fig. S7a and densitometric quantification in Fig. S7b). The intensity of GH-signals in the AP is slightly lower in *Reck* $^{+/-}$ mice, normal in Hypo mice, and substantially lower in TAX-treated iKO mice (Fig. S7b). Hence, somatotrophs seem to be intact in Hypo mice but are affected in TAX-treated iKO mice.

The concentration of plasma GH in four groups of mice is shown in Fig. S7c. Due to the large inter-animal variation, significant difference between the groups could not be detected, but the average GH

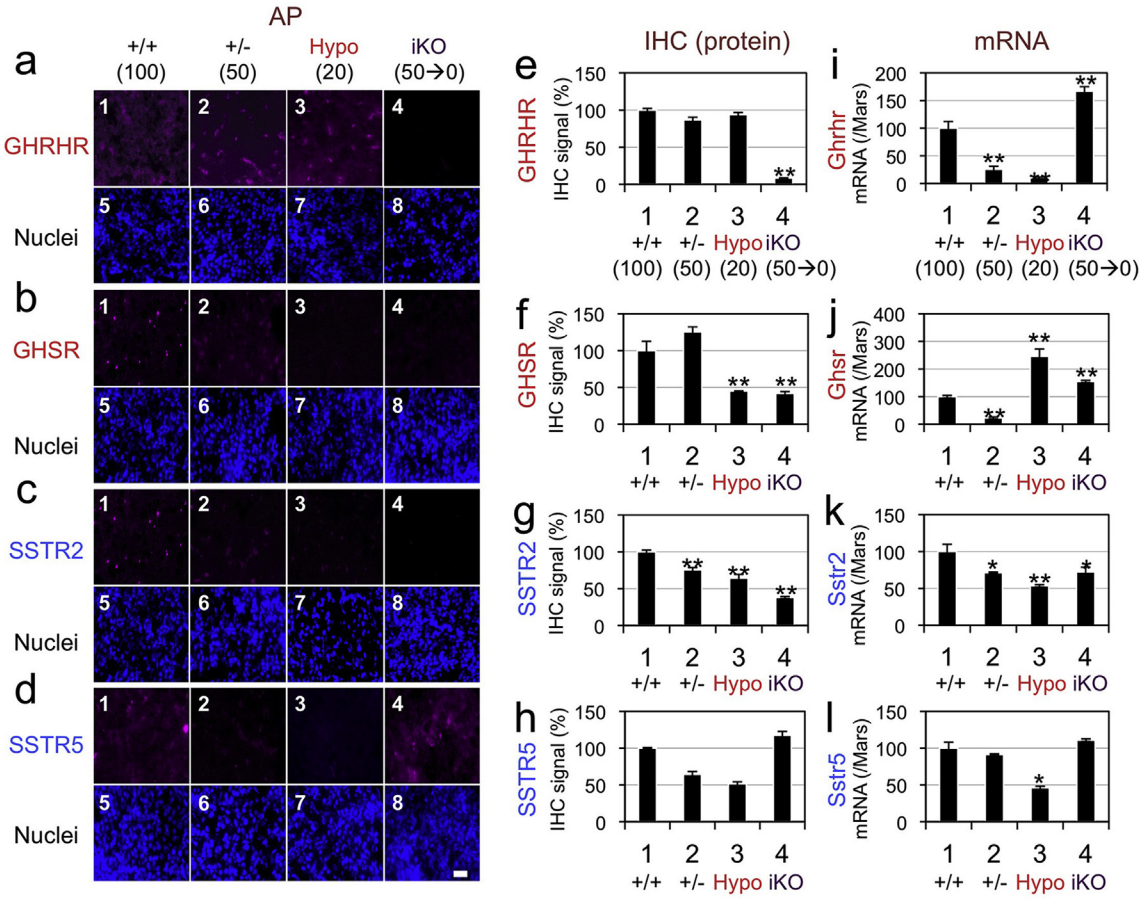

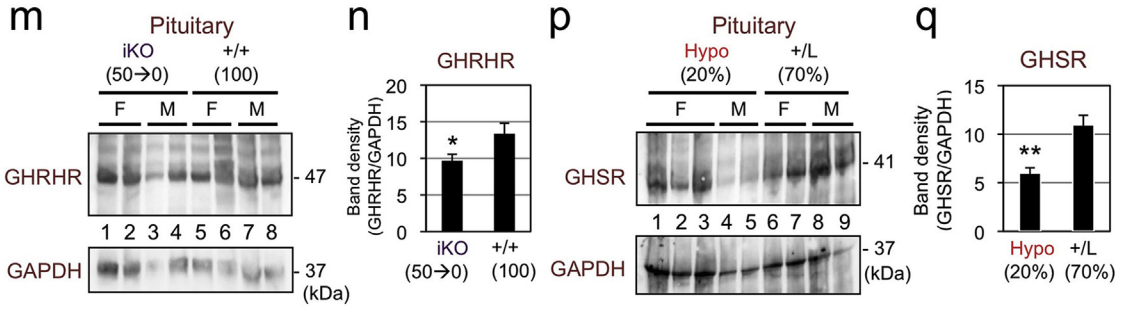

o

GHRHR	iKO	+/+	P
Male	10.3	12.8	0.23
Female	9.1	13.9	0.11
Both	9.7	13.4	0.035

r

GHSR	Hypo	+/L	P
Male	4.9	11.9	0.035
Female	6.7	10.0	0.016
Both	4.2	7.5	0.0011

Fig. 4. Effects of *Reck* mutations on four GPCRs involved in the regulation of GH-secretion from somatotrophs. (**a–d**) Immunofluorescence staining of AP sections from four groups of female mice using antibodies against two stimulatory GPCRs [GHRHR **(a)** and GHSR **(b)**] and two inhibitory GPCRs [SSTR2 **(c)** and SSTR5 **(d)**]. Representative immunofluorescence images (1–4) and the corresponding nuclear images (5–8) are shown. Scale bar: 50 μm. **(e–h)** Intensity of immunofluorescence signals for the indicated receptors in AP sections from four groups of female mice (n ≥ 4). Integrated density of far-red fluorescence in the images such as those shown in **a-d** was determined using Fiji software. **(i–l)** The levels of the indicated mRNA in the AP from four groups of female mice (n ≥ 4). Total RNA extracted from the AP was subjected to qRT-PCR using the primer sets listed in Table S2. The data were normalized against the house-keeping gene *Mars* (Methionyl-tRNA synthetase). The significance of the differences among four groups of data was assessed by one-way ANOVA and the Mann–Whitney *U* test (see Fig. S9); when appropriate, the significance of the differences between the wild type group and each mutant group was assessed by Student's T-test (*P < 0.05, **P < 0.01). The findings are summarized in Fig. 6a (blue shading). **(m–p)** Effects of *Reck* on GHRHR **(m–o)** and GHSR **(p–r)** expressed in the pituitary gland. Lysates of pituitary glands were prepared from the indicated mice and subjected to immunoblot assay using anti-GHRHR (**m**, upper panel) or anti-GHSR (**p**, upper panel) followed by re-probing of the same blot with anti-GAPDH (**m**, **p**, lower panels, respectively). F: female. M: male. Results of the densitometric quantification of the data shown in **m** and **p**, normalized against GAPDH, are summarized in **n** and **q**, respectively. Bar: mean ± sem. *P = 0.035, **P = 0.0011. The data (average band density and P-value) for males and females (n = 2) are separately shown in **o** and **r**.

concentration seems to be higher in the three *Reck* mutants compared to the normal mice (Fig. S7c, solid bars). Fasting is known to elevate the level of plasma GH in mice (Luque et al., 2007). After fasting for 16 h (Fig. S7c, open bars), the average GH concentration was indeed increased in normal mice as well as in *Reck* $^{+/-}$ mice. Interestingly, however, fasting seems to have little influence on GH concentration in Hypo mice and fasting appeared to decrease GH concentration in TAX-treated iKO mice. Although very preliminary, these data suggest that RECK may influence GH secretion and its response to fasting. Since the average GH level in the TAX-treated iKO mice fed ad libitum was higher than in normal mice (Fig. S7c, bars 7 vs. 1), the dramatic decrease in GH immunoreactivity found in the AP of TAX-treated iKO mice (Fig. S7a, panel 8; Fig. S7b) might not represent a large decrease in the number of somatotrophs but rather an alteration in some property of the somatotrophs in these animals, for example an increase in the GH secretion/GH expression ratio.

3.4. Responses of Reck mutant mice to GHRP-2 and octreotide

We also tested the effects of two synthetic peptides, GHRP-2 (GHSR agonist) and Octreotide (SSTR2 agonist), on circulating GH in these mice. It is known that GHRP-2 stimulates and Octreotide inhibits GH secretion. Peripheral blood samples were collected before and 30 min after injection of either GHRP-2 or Octreotide, and the plasma GH concentration was determined (Fig. S8c, d; data summarized in Fig. S7d, e). Interestingly, Hypo mice showed increased sensitivity to GHRP-2 (Fig. S7d, bar 3), and TAX-treated iKO mice showed increased sensitivity to Octreotide (Fig. S7e, bar 5). Thus, RECK may affect the sensitivity of somatotrophs to these peptides. These findings prompted us to determine and compare the levels of relevant hormone receptors expressed on somatotrophs in these mice.

3.5. Reck affects the levels of several GPCRs expressed in the AP

Pituitary slices prepared from the four lines of mice were subjected to immunofluorescence staining with antibodies against two stimulatory hormone receptors (GHRHR, GHSR) and two inhibitory hormone receptors (SSTR2, SSTR5) expressed on somatotrophs (Fig. 4a–d), and the fluorescence intensity of the images acquired under comparable conditions was quantified (Fig. 4e–h; Fig. S9e-h). All these hormone receptors belong to the GPCR family. We also extracted total RNA from the AP and estimated the levels of mRNAs encoding these hormone receptors by quantitative reverse transcription-polymerase chain reaction (qRT-PCR) (Fig. 4i-l; Fig. S9i-l).

When RECK was constitutively reduced to half or to ~20% of the normal level (i.e., *Reck* $^{+/-}$ or Hypo), the stimulatory hormone receptor GHRHR was downregulated at the mRNA level (Fig. 4i, bars 2, 3) but unchanged at the immunoreactivity level (Fig. 4e, bars 2, 3). This is in sharp contrast to TAX-treated iKO mice in which GHRHR was dramatically decreased at the immunoreactivity level (Fig. 4e, bar 4) but increased at the mRNA level (Fig. 4i, bar 4).

The other stimulatory hormone receptor GHSR showed a similar

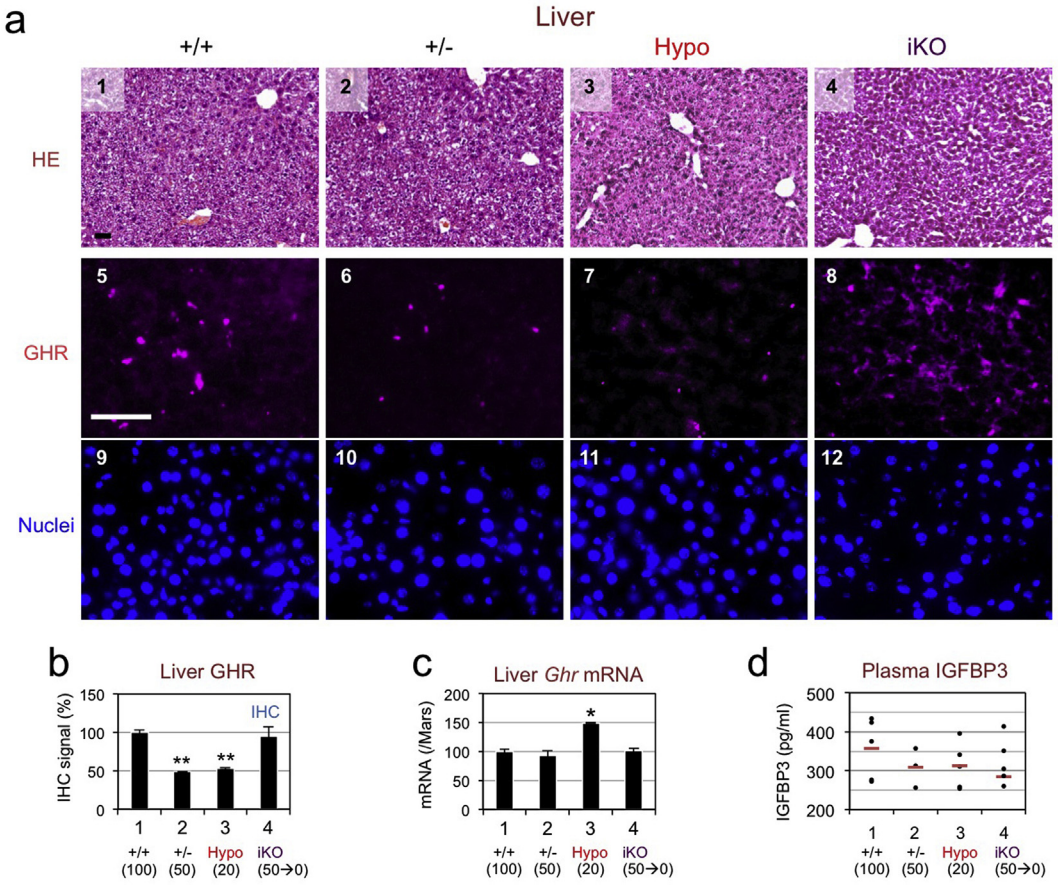

Fig. 5. Evaluation of liver GHR and plasma IGFBP3. (a) Histology of the liver. Slices of the liver from the indicated mice (female) were subjected to HE staining (panels 1–4) or immunofluorescence staining with anti-GHR antibodies (panels 5–8) followed by nuclear counter-staining (panels 9–12). Typical images from about the same areas in the liver are shown. Scale bar (50 μm) in panel 1 is for panels 1–4, and that in panel 5 is for panels 5–12. **(b)** Intensity of GHR-immunofluorescence signals in liver sections from four groups of female mice (n = 4). Integrated density of far-red fluorescence in the images such as those shown in **a** was determined using the Fiji software. **(c)** The levels of *Ghr* mRNA in the liver from four groups of mice (n ≥ 2). Total RNA extracted from the liver was subjected to qRT-PCR using the primer sets listed in Table S2 and normalized against Mars. **(d)** Plasma IGFBP3 in four groups of female mice (15–18 weeks after birth).

pattern to GHRHR expression in *Reck* $^{+/-}$ mice, decreased mRNA and unchanged immunoreactivity (Fig. 4j, f, bar 2). This contrasts with GHSR in Hypo and TAX-treated iKO mice in which GHSR was decreased at the immunoreactivity level but increased at the mRNA level (Fig. 4f, j).

The level of the inhibitory hormone receptor SSTR2 was decreased at both the immunoreactivity and mRNA levels in *Reck*$^{+/-}$, Hypo, and TAX-treated iKO mice (Fig. 4g, k). Expression of the other inhibitory hormone receptor, SSTR5, in *Reck* $^{+/-}$ and Hypo mice was similar to that of SSTR2 (Fig. 4h, l). However, expression of SSTR5 in TAX-treated iKO mice was not different from the control mice (Fig. 4h, l, bar 4). These observations are summarized in Fig. 6a, and our interpretations are described in the Discussion.

We also performed immunoblot assays for the two stimulatory receptors using pituitary gland lysates (Fig. 4m, p). This assay is technically challenging since the organ is small (the amount of protein per sample is limited) and mild conditions are necessary to solubilize GPCRs. Nevertheless, we could detect decreases in the intensity of the GHRHR band in samples from TAX-treated mice (Fig. 4m–o) and decreases in the intensity of the GHSR band in samples from Hypo mice (Fig. 4p–r). Thus, the results obtained from immunofluorescent staining of AP tissue slices are in accord with the results of the immunoblot assays.

3.6. Growth hormone receptor (GHR) in the liver

A major target organ of circulating GH is the liver where the hormone binds GHR and transduces signals to stimulate IGF1 production (Dehkhoda et al., 2018). RECK is detectable in the liver of adult mice (Fig. S10, lane 2). We therefore performed immunofluorescence staining and qRT-PCR to characterize GHR expressed in the liver of normal and *Reck* mutant mice (Fig. 5a–c; Fig. S6b). In *Reck* $^{+/-}$ mice, GHR was decreased at the immunoreactivity level (Fig. 5b, bar 2) but not at the mRNA level (Fig. 5c, bar 2). In Hypo mice, on the other hand, GHR was decreased at the immunoreactivity level (Fig. 5b, bar 3) but increased at the mRNA level (Fig. 5c, bar 3). In TAX-treated iKO mice, the amount of GHR was comparable to that in normal mice both at the immunoreactivity and mRNA levels (Fig. 5b and c, bar 4). The results are summarized in Fig. 6a, and our interpretations are described in the Discussion.

Since IGF binding protein-3 (IGFBP3) is known to be important in maintaining circulating IGF1 (Ohlsson et al., 2009), we determined the levels of IGFBP3 in the plasma of these mice (Fig. 5d). There were no significant differences in plasma IGFBP3 levels between any of the mutant mice and normal mice (Fig. S6c).

4. Discussion

In the mouse embryo, *Reck* is expressed in multiple tissues and is critical for development and survival (Oh et al., 2001; Echizenya et al., 2005; Kondo et al., 2007; Muraguchi et al., 2007; Chandana et al., 2010; Yamamoto et al., 2012; Almeida et al., 2015; Cho et al., 2017). In contrast, *Reck* expression in adult mice is found only in restricted areas (e.g., see Fig. 1), and the mouse is viable when *Reck*-deletion is induced (at an efficiency of ~74%) generating mice that express RECK at approximately 13% of normal as early as 10 days after birth (i.e., TAX-treated iKO mice). Thus, near the end of embryogenesis or during early postnatal life, a transition in the role of RECK from a regulator of systemic tissue remodeling to a more specialized function seems to takes place.

A clue to the biological function of a gene may be obtained from the pattern of its expression in the body. Using two *Reck* reporter lines recently developed (Fig. S1) (Matsuzaki et al., 2018b) we initially found that RECK is expressed in two small regions in the basal part of mouse brain: the ARH and AP (Fig. 1). Our data also suggest that a large proportion of somatotrophs express *Reck*.

A more direct approach to understanding the biological functions of a gene is to inactivate the gene in animals. In the case of *Reck*, however, complete inactivation in mice results in embryonic death and thus provides no clue to its functions in postnatal life. To circumvent this obstacle, we employed two viable *Reck* mutant lines in this study: Hypo and iKO. An important feature of Hypo mice is that the level of RECK expression is chronically and uniformly low (~20% of the normal level) throughout their lives. However, the limb abnormalities (Yamamoto et al., 2012) and possible developmental adaptation/compensation to the chronic shortage of RECK in Hypo mice may complicate the interpretation of experimental results. The iKO mutant, on the other hand, expresses RECK at approximately 50% of normal, and the *RECK* $^{\pm}$ line, which also expresses RECK at 50% of normal, has no apparent defects. The iKO mouse can be treated with TAX to reduce RECK expression to approximately 13% of normal (see Results section 3.2). When iKO mice are treated with TAX on or after P10, developmental adaptation/compensation to low RECK expression is expected to be milder than in the Hypo mouse. A drawback of the iKO mouse, however, is that the efficiency of gene deletion is not 100% and cells that continue to express RECK (approximately 26% of originally RECK-positive cells in the case

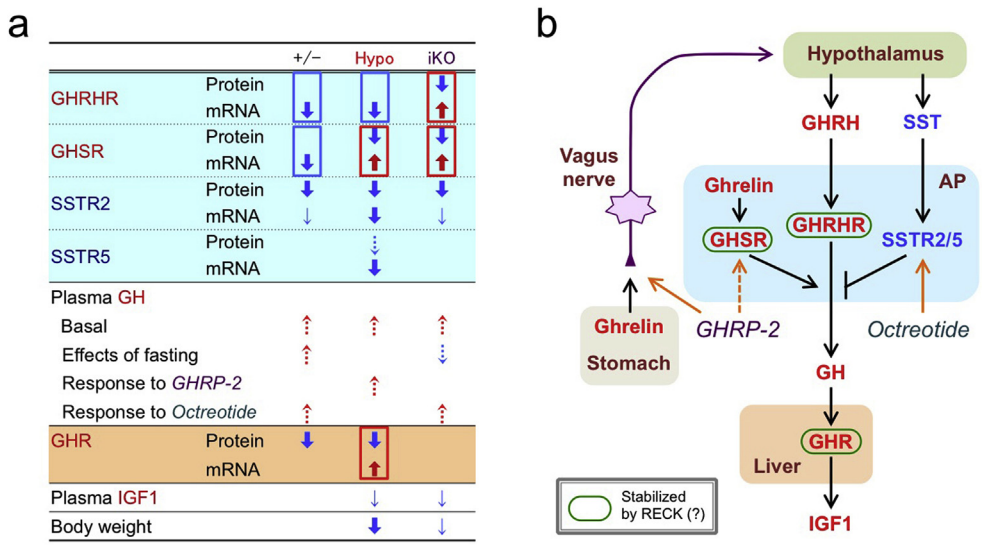

Fig. 6. Summary of our findings. (a) Summary of the results. Red upward arrow indicates increase and blue downward arrow decrease from the control. Broken arrows in the "Plasma GH" section do not represent statistical significance. In other sections, thin arrows correspond to $P < 0.05$, and thick arrows to $P < 0.01$ (Student's t-test). Red boxes indicate a proposed causative alteration contributing to the phenotype (reduced IGF1, body weight, and body length). Blue boxes indicate possible protein stabilization. **(b)** Key molecules in the GH/IGF1 axis. Sites of actions of two synthetic peptides, GHRP-2 and Octreotide, are also shown. Colored areas (green, blue, yellow, and orange) signify different organs. Molecules playing positive roles in this pathway are in red, while those playing negative roles are in blue. Arrows indicate stimulation and T-shaped bars inhibition. Colored areas in **a** correspond to the organs similarly colored in **b**.

of the AP) may complicate the interpretation of experimental results. We therefore reasoned that the comparison of these two mutant lines that had been made RECK deficient by different strategies could lead us to a better understanding of the role for RECK in postnatal mice. Importantly, Hypo and TAX-treated iKO mutants share a similar set of phenotypes: decreased body sizes and lower plasma IGF1 levels than the control mice.

The sites of abundant *Reck* expression in adult mice (i.e., the ARH and somatotrophs) and the reduced IGF1 levels in these *Reck* mutant mice raised the obvious possibility that RECK influences body size by affecting GH production. We tested this hypothesis by comparing the expression of GH in the AP (Fig. S7a, b) and the levels of circulating GH in untreated mice (Fig. S7c, solid bar), the effects of fasting on the levels of circulating GH (Fig. S7c, open bar), the effects of two synthetic peptides (GHRP-2, octreotide) on the levels of circulating GH (Fig. S7d, e; Fig. S8c, d), the status of several membrane receptors involved in the regulation of GH secretion in the AP (Fig. 4), and the expression of GHR in the liver (Fig. 5a–c) between control and *Reck* mutant mice. The results are schematically summarized in Fig. 6a. In the case of Hypo mice, alterations in two molecules are notable: decreased immunoreactivity of two proteins, GHSR in the AP and GHR in the liver, with concomitant increases in their mRNAs (see red boxes in the column "Hypo" in Fig. 6a). Our immunoblot data (Fig. 4p–r) confirm that the decrease in GHSR immunoreactivity in the AP represents a decrease in the amount of this protein. In the case of TAX-treated iKO mice, the decreases in the immunoreactivity of two proteins, GHRHR and GHSR in the AP, again with concomitant increases in their mRNAs were noted (see red boxes in the column "iKO" in Fig. 6a). Our immunoblot data (Fig. 4m–o) confirm that the decrease in GHRHR immunoreactivity represents a decrease in the amount of this protein. These findings implicate RECK in keeping the amounts of some of the membrane receptors involved in the GH/IGF1 axis at proper levels.

How can the phenotype of each *Reck* mutant line be explained? Given the known function of RECK as a membrane-anchored regulator of metalloproteinases, it is reasonable to speculate that reduced immunoreactivity and a reduced immunoblot band of a membrane protein in *Reck* mutant mice represent degradation of that protein. The previous observations that liver-specific knockout of *Igf1* gene results in upregulation of *Ghrhr* and *Ghsr* gene expression in the AP (Sjogren et al., 2002) suggest that IGF1 mediates negative feedback regulation of these genes. Hence, the decreased immunoreactivities of GHRHR and/or GHSR with concomitant increase in corresponding mRNA(s) found in Hypo and TAX-treated iKO mice (red boxes in the blue area in Fig. 6a) may represent degradation of these GPCRs followed by feedback upregulation of mRNA(s) triggered, for example, by the decrease in IGF1. On the other hand, the decrease in *Ghrhr*, *Ghsr*, and *Sstr5* mRNA with no change in immunoreactivity found in *Reck* $^{+/-}$ and Hypo mice (blue boxes in Fig. 6a) may represent protein stabilization by unknown mechanisms to cope with reduced RECK. Taking these into account, the phenotypes of each mutant may be explained as follows (Fig. 6b; Fig. S11):

[1] In *Reck* $^{+/-}$ mice, GHR expression in the liver is reduced, but this effect is masked by feedback mechanisms, such as stabilization of two stimulatory hormone receptors GHRHR and GHSR in the AP, preventing the decreases in body weight and IGF1 secretion.
[2] In Hypo mice, GHR in the liver is further reduced (degraded) while GHSR is also reduced (degraded) in the AP, making it impossible to mask the effects of GHR reduction and hence leading to reduced IGF1 secretion.
[3] In TAX-treated iKO mice, two stimulatory hormone receptors, GHRHR and GHSR, in the AP are both decreased (degraded), leading to reduced GH secretion and reduced IGF1 secretion, although GHR reduction has been reversed by an unknown mechanism.

Our results, however, do not exclude other possibilities, such as a role for RECK in signal transduction downstream of these receptors, or in growth and/or differentiation of somatotrophs. Since all the *Reck* mutants employed in this study are non-tissue-specific, it is possible that the reduction of RECK in tissues that we are not focusing on is responsible for the observed phenotypes. To clarify this point, mice with selective *Reck* inactivation in specific tissues, such as the AP, ARH, vagus nerve, and liver, need to be established and studied. In this study, we focused on *Reck*-expressing cells in the AP and the phenotypes of female mutant mice. The *Reck*-expressing cells in the ARH (where GHRH-producing neurons resides among others) and the phenotypes of male mutant mice (where pulsatile GH secretion is more prominent) need to be examined in future studies. Likewise, our findings at the protein level led us to focus on the positive regulators of GH secretion in this study. In fact, however, it was the level of SSTR2 protein (Fig. 4g; Fig. S9g) that shows the best correlation with the levels of RECK protein. The reason for this correlation and the mechanisms by which Hypo and TAX-treated iKO mutations act differently on *Sstr5* mRNA in the AP (bars 3 and 4 in Fig. 4l) and GHR in the liver (Fig. 5b) are among the interesting questions to be addressed in future studies.

Nevertheless, our finding that the non-tissue-specific manipulation of *Reck* expression results in marked phenotypes relevant to the GH/IGF1 axis may have important clinical implications. Although RECK has been studied as a tumor suppressor, epigenetically inactivated in a wide variety of cancers, its contributions to somatic growth and metabolisms have been unappreciated. For instance, a single nucleotide polymorphism (SNP) in the RECK promoter region, which is likely to affect the level of RECK expression, has been implicated in susceptibility to certain tumors. Whether a similar correlation will be detected among people with GH/IGF1 axis-related disorders is an issue worthy of investigation.

5. Conclusions and future directions

Reck is expressed in somatotrophs in adult mice. Two viable *Reck* mutants, one with greatly reduced *Reck* expression and the other with postnatal *Reck* inactivation, exhibit common phenotypes of reduced body size and lower plasma IGF1 levels compared to control mice. Our experimental data suggest that the GH/IGF1 axis is affected in these mutant mice, although the molecular mechanisms by which RECK affects this endocrine regulatory pathway needs to be further clarified in future studies.

CRediT authorship contribution statement

Shuichiro Ogawa: Conceptualization, Methodology, Validation, Formal analysis, Investigation, Data curation, Writing - original draft, Writing - review & editing, Visualization. **Tomoko Matsuzaki:** Conceptualization, Methodology, Validation, Formal analysis, Investigation, Data curation, Writing - original draft, Writing - review & editing, Visualization, Project administration. **Makoto Noda:** Conceptualization, Methodology, Formal analysis, Data curation, Writing - review & editing, Visualization, Supervision, Project administration, Funding acquisition.

Declaration of competing interest

Authors have no conflicts of interest to declare.

Acknowledgments

This work was supported by KAKENHI (JSPS-16GS0311 and MEXT-22123005).We are grateful to Dr. Pierre Chambon for Cre-ERT2 plasmid, Dr. Philippe Soriano for R26R mice, Drs. Liqun Luo and Ryoichiro Kageyama for mTmG mice, Drs. Masayasu Kojima, Tatsuaki

Tsuruyama, Glicia Almeida, and Keiko Iwaisako for scientific and technical advices, Drs. Seiho Nagafuchi, Takeshi Usui, and Kazuwa Nakao for discussions on clinical aspects, Sachiyo Yamaguchi for her help in producing data shown in Fig. S10, Emi Nishimoto, Hai-Ou Gu, Mika Fujiwara, and Kumi Kawade for technical assistance, Aki Miyazaki for administrative assistance, and Dr. David B. Alexander for critical reading of the manuscript.

Appendix A. Supplementary data

Supplementary data related to this article can be found at https://doi.org/10.1016/j.mce.2020.110790.

References

Almeida, G.M., Yamamoto, M., Morioka, Y., Ogawa, S., Matsuzaki, T., Noda, M., 2015. Critical roles for murine Reck in the regulation of vascular patterning and stabilization. Sci. Rep. 5, 17860.
Ben-Shlomo, A., Melmed, S., 2010. Pituitary somatostatin receptor signaling. Trends Endocrinol. Metab. 21, 123–133.
Berelowitz, M., Szabo, M., Frohman, L.A., Firestone, S., Chu, L., Hintz, R.L., 1981. Somatomedin-C mediates growth hormone negative feedback by effects on both the hypothalamus and the pituitary. Science 212, 1279–1281.
Chandana, E.P., Maeda, Y., Ueda, A., Kiyonari, H., Oshima, N., Yamamoto, M., Kondo, S., Oh, J., Takahashi, R., Yoshida, Y., Kawashima, S., Alexander, D.B., Kitayama, H., Takahashi, C., Tabata, Y., Matsuzaki, T., Noda, M., 2010. Involvement of the Reck tumor suppressor protein in maternal and embryonic vascular remodeling in mice. BMC Dev. Biol. 10, 84.
Cho, C., Smallwood, P.M., Nathans, J., 2017. Reck and Gpr124 are essential receptor cofactors for wnt7a/wnt7b-specific signaling in mammalian CNS angiogenesis and blood-brain barrier regulation. Neuron 95, 1221–1225.
Date, Y., Murakami, N., Toshinai, K., Matsukura, S., Niijima, A., Matsuo, H., Kangawa, K., Nakazato, M., 2002. The role of the gastric afferent vagal nerve in ghrelin-induced feeding and growth hormone secretion in rats. Gastroenterology 123, 1120–1128.
Date, Y., Shimbara, T., Koda, S., Toshinai, K., Ida, T., Murakami, N., Miyazato, M., Kokame, K., Ishizuka, Y., Ishida, Y., Kageyama, H., Shioda, S., Kangawa, K., Nakazato, M., 2006. Peripheral ghrelin transmits orexigenic signals through the noradrenergic pathway from the hindbrain to the hypothalamus. Cell Metabol. 4, 323–331.
Dauber, A., Rosenfeld, R.G., Hirschhorn, J.N., 2014. Genetic evaluation of short stature. J. Clin. Endocrinol. Metab. 99, 3080–3092.
Dehkhoda, F., Lee, C.M.M., Medina, J., Brooks, A.J., 2018. The growth hormone receptor: mechanism of receptor activation, cell signaling, and physiological aspects. Front. Endocrinol. 9, 35.
Denef, C., 2008. Paracrinicity: the story of 30 years of cellular pituitary crosstalk. J. Neuroendocrinol. 20, 1–70.
Echizenya, M., Kondo, S., Takahashi, R., Oh, J., Kawashima, S., Kitayama, H., Takahashi, C., Noda, M., 2005. The membrane-anchored MMP-regulator RECK is a target of myogenic regulatory factors. Oncogene 24, 5850–5857.
Eigler, T., Ben-Shlomo, A., 2014. Somatostatin system: molecular mechanisms regulating anterior pituitary hormones. J. Mol. Endocrinol. 53, R1–R19.
Eubelen, M., Bostaille, N., Cabochette, P., Gauquier, A., Tebabi, P., Dumitru, A.C., Koehler, M., Gut, P., Alsteens, D., Stainier, D.Y.R., Garcia-Pino, A., Vanhollebeke, B., 2018. A molecular mechanism for Wnt ligand-specific signaling. Science 361, eatt1178.
Forni, P.E., Scuoppo, C., Imayoshi, I., Taulli, R., Dastru, W., Sala, V., Betz, U.A., Muzzi, P., Martinuzzi, D., Vercelli, A.E., Kageyama, R., Ponzetto, C., 2006. High levels of Cre expression in neuronal progenitors cause defects in brain development leading to microencephaly and hydrocephaly. J. Neurosci. 26, 9593–9602.
Fridlyand, L.E., Tamarina, N.A., Schally, A.V., Philipson, L.H., 2016. Growth hormone-releasing hormone in diabetes. Front. Endocrinol. 7, 129.
Gadelha, M.R., Kasuki, L., Korbonits, M., 2012. Novel pathway for somatostatin analogs in patients with acromegaly. Trends Endocrinol. Metab. 24, 238–246.
Gahete, M.D., Luque, R.M., Castano, J.P., 2016. Models of GH deficiency in animal studies. Best Pract. Res. Clin. Endocrinol. Metabol. 30, 693–704.
Higashi, A.Y., Ikawa, T., Muramatsu, M., Economides, A.N., Niwa, A., Okuda, T., Murphy, A.J., Rojas, J., Heike, T., Nakahata, T., Kawamoto, H., Kita, T., Yanagita, M., 2009. Direct hematological toxicity and illegitimate chromosomal recombination caused by the systemic activation of CreERT2. J. Immunol. 182, 5633–5640.
Hill, V.K., Ricketts, C., Bieche, I., Vacher, S., Gentle, D., Lewis, C., Maher, E.R., Latif, F., 2011. Genome-wide DNA methylation profiling of CpG islands in breast cancer identifies novel genes associated with tumorigenicity. Canc. Res. 71, 2988–2999.
Howard, A.D., Feighner, S.D., Cully, D.F., Arena, J.P., Liberator, P.A., Rosenblum, C.I., Hamelin, M., Hreniuk, D.L., Palyha, O.C., Anderson, J., Paress, P.S., Diaz, C., Chou, M., Liu, K.K., McKee, K.K., Pong, S.S., Chaung, L.Y., Elbrecht, A., Dashkevicz, M., Heavens, R., Rigby, M., Sirinathsinghji, D.J., Dean, D.C., Melillo, D.G., Patchett, A.A., Nargund, R., Griffin, P.R., DeMartino, J.A., Gupta, S.K., Schaeffer, J.M., Smith, R.G., Van der Ploeg, L.H., 1996. A receptor in pituitary and hypothalamus that functions in growth hormone release. Science 273, 974–977.
Jansson, J.O., Eden, S., Isaksson, O., 1985. Sexual dimorphism in the control of growth hormone secretion. Endocr. Rev. 6, 128–150.
Ketha, H., Singh, R.J., 2015. Clinical assays for quantitation of insulin-like-growth-factor-1 (IGF1). Methods 81, 93–98.
Kojima, M., Hosoda, H., Date, Y., Nakazato, M., Matsuo, H., Kangawa, K., 1999. Ghrelin is a growth-hormone-releasing acylated peptide from stomach. Nature 402, 656–660.
Kojima, M., Kangawa, K., 2005. Ghrelin: structure and function. Physiol. Rev. 85, 495–522.
Kondo, S., Shukunami, C., Morioka, Y., Matsumoto, N., Takahashi, R., Oh, J., Atsumi, T., Umezawa, A., Kudo, A., Kitayama, H., Hiraki, Y., Noda, M., 2007. Dual effects of the membrane-anchored MMP regulator RECK on chondrogenic differentiation of ATDC5 cells. J. Cell Sci. 120, 849–857.
Laron, Z., 1999. Somatomedin-1 (recombinant insulin-like growth factor-1): clinical pharmacology and potential treatment of endocrine and metabolic disorders. BioDrugs 11, 55–70.
Luque, R.M., Park, S., Kineman, R.D., 2007. Severity of the catabolic condition differentially modulates hypothalamic expression of growth hormone-releasing hormone in the fasted mouse: potential role of neuropeptide Y and corticotropin-releasing hormone. Endocrinology 148, 300–309.
Matsuzaki, T., Kitayama, H., Omura, A., Nishimoto, E., Alexander, D., Noda, M., 2018a. The RECK tumor suppressor protein binds and stabilizes ADAMTS10. Biol. Open 7, bio033985.
Matsuzaki, T., Wang, H., Imamura, Y., Kondo, S., Ogawa, S., Noda, M., 2018b. Generation and characterization of a mouse line carrying Reck-CreERT2 knock-in allele. Genesis 56, e23099.
Melmed, S., 2011. Pathogenesis of pituitary tumors. Nat. Rev. Endocrinol. 7, 257–266.
Melmed, S., 2016. New therapeutic agents for acromegaly. Nat. Rev. Endocrinol. 12, 90–98.
Mitrofanova, L.B., Konovalov, P.V., Krylova, J.S., Polyakova, V.O., Kvetnoy, I.M., 2017. Plurihormonal cells of normal anterior pituitary: facts and conclusions. Oncotarget 8, 29282–29299.
Muraguchi, T., Takegami, Y., Ohtsuka, T., Kitajima, S., Chandana, E.P., Omura, A., Miki, T., Takahashi, R., Matsumoto, N., Ludwig, A., Noda, M., Takahashi, C., 2007. RECK modulates Notch signaling during cortical neurogenesis by regulating ADAM10 activity. Nat. Neurosci. 10, 838–845.
Muzumdar, M.D., Tasic, B., Miyamichi, K., Li, L., Luo, L., 2007. A global double-fluorescent Cre reporter mouse. Genesis 45, 593–605.
Noda, M., Oh, J., Takahashi, R., Kondo, S., Kitayama, H., Takahashi, C., 2003. RECK: a novel suppressor of malignancy linking oncogenic signaling to extracellular matrix remodeling. Canc. Metastasis Rev. 22, 167–175.
Noda, M., Takahashi, C., 2007. Recklessness as a hallmark of aggressive cancer. Canc. Sci. 98, 1659–1665.
Noda, M., Vallon, M., Kuo, C.J., 2016. The Wnt7's Tale: a story of an orphan who finds her tie to a famous family. Canc. Sci. 107, 12924.
Oh, J., Takahashi, R., Kondo, S., Mizoguchi, A., Adachi, E., Sasahara, R.M., Nishimura, S., Imamura, Y., Kitayama, H., Alexander, D.B., Ide, C., Horan, T.P., Arakawa, T., Yoshida, H., Nishikawa, S., Itoh, Y., Seiki, M., Itohara, S., Takahashi, C., Noda, M., 2001. The membrane-anchored MMP inhibitor RECK is a key regulator of extracellular matrix integrity and angiogenesis. Cell 107, 789–800.
Ohlsson, C., Mohan, S., Sjogren, K., Tivesten, A., Isgaard, J., Isaksson, O., Jansson, J.O., Svensson, J., 2009. The role of liver-derived insulin-like growth factor-I. Endocr. Rev. 30, 494–535.
Omura, A., Matsuzaki, T., Mio, K., Ogura, T., Yamamoto, M., Fujita, A., Okawa, K., Kitayama, H., Takahashi, C., Sato, C., Noda, M., 2009. RECK forms cowbell-shaped dimers and inhibits matrix metalloproteinase-catalyzed cleavage of fibronectin. J. Biol. Chem. 284, 3461–3469.
Peroni, C.N., Hayashida, C.Y., Nascimento, N., Longuini, V.C., Toledo, R.A., Bartolini, P., Bowers, C.Y., Toledo, S.P., 2012. Growth hormone response to growth hormone-releasing peptide-2 in growth hormone-deficient little mice. Clinics 67, 265–272.
Pilecka, I., Whatmore, A., Hooft van Huijsduijnen, R., Destenaves, B., Clayton, P., 2007. Growth hormone signalling: sprouting links between pathways, human genetics and therapeutic options. Trends Endocrinol. Metab. 18, 12–18.
Ranke, M.B., Wit, J.M., 2018. Growth hormone - past, present and future. Nat. Rev. Endocrinol. 14, 285–300.
Shi, G., Yoshida, Y., Yuki, K., Nishimura, T., Kawata, Y., Kawashima, M., Iwaisako, K., Yoshikawa, K., Kurebayashi, J., Toi, M., Noda, M., 2016. Pattern of RECK CpG methylation as a potential marker for predicting breast cancer prognosis and drug-sensitivity. Oncotarget 7, 8620.
Sjogren, K., Jansson, J.O., Isaksson, O.G., Ohlsson, C., 2002. A model for tissue-specific inducible insulin-like growth factor-I (IGF-I) inactivation to determine the physiological role of liver-derived IGF-I. Endocrine 19, 249–256.
Soriano, P., 1999. Generalized lacZ expression with the ROSA26 Cre reporter strain. Nat. Genet. 21, 70–71.
Takahashi, C., Sheng, Z., Horan, T.P., Kitayama, H., Maki, M., Hitomi, K., Kitaura, Y., Takai, S., Sasahara, R.M., Horimoto, A., Ikawa, Y., Ratzkin, B.J., Arakawa, T., Noda, M., 1998. Regulation of matrix metalloproteinase-9 and inhibition of tumor invasion by the membrane-anchored glycoprotein RECK. Proc. Natl. Acad. Sci. U. S. A. 95, 13221–13226.
Ulrich, F., Carretero-Ortega, J., Menendez, J., Narvaez, C., Sun, B., Lancaster, E., Pershad, V., Trzaska, S., Veliz, E., Kamei, M., Prendergast, A., Kidd, K.R., Shaw, K.M., Castranova, D.A., Pham, V.N., Lo, B.D., Martin, B.L., Raible, D.W., Weinstein, B.M., Torres-Vazquez, J., 2016. Reck enables cerebrovascular development by promoting canonical Wnt signaling. Development 143, 147–159.
Vallon, M., Yuki, K., Nguyen, T.D., Chang, J., Yuan, J., Siepe, D., Miao, Y., Essler, M., Noda, M., Garcia, K.C., Kuo, C.J., 2018. A RECK-WNT7 receptor-ligand interaction enables isoform-specific regulation of wnt bioavailability. Cell Rep. 25 339-349 e339.
Vanhollebeke, B., Stone, O.A., Bostaille, N., Cho, C., Zhou, Y., Maquet, E., Gauquier, A., Cabochette, P., Fukuhara, S., Mochizuki, N., Nathans, J., Stainier, D.Y., 2015. Tip

cell-specific requirement for an atypical Gpr124- and Reck-dependent Wnt/beta-catenin pathway during brain angiogenesis. Elife 4. https://doi.org/10.7554/eLife.06489.

Wallenius, K., Sjogren, K., Peng, X.D., Park, S., Wallenius, V., Liu, J.L., Umaerus, M., Wennbo, H., Isaksson, O., Frohman, L., Kineman, R., Ohlsson, C., Jansson, J.O., 2001. Liver-derived IGF-I regulates GH secretion at the pituitary level in mice. Endocrinology 142, 4762–4770.

Yamamoto, M., Matsuzaki, T., Takahashi, R., Adachi, E., Maeda, Y., Yamaguchi, S., Kitayama, H., Echizenya, M., Morioka, Y., Alexander, D.B., Yagi, T., Itohara, S., Nakamura, T., Akiyama, H., Noda, M., 2012. The transformation suppressor gene Reck is required for postaxial patterning in mouse forelimbs. Biol. Open 1, 458–466.

Yamashita, S., Melmed, S., 1987. Insulinlike growth factor I regulation of growth hormone gene transcription in primary rat pituitary cells. J. Clin. Invest. 79, 449–452.